Du, B.; Handge, U.A.; Majeed, S.; Abetz, V..:
Localization of functionalized MWCNT in SAN/PPE blends and their influence on rheological properties
In: Polymer (2012) Elsevier

DOI: 10.1016/j.polymer.2012.09.047

Localization of functionalized MWCNT in SAN/PPE blends and their influence on rheological properties

Bing Du, Ulrich A. Handge, Shahid Majeed, Volker Abetz*
Institute of Polymer Research, Helmholtz-Zentrum Geesthacht
Max-Planck-Strasse 1, 21502 Geesthacht, Germany

Abstract

In this work, the morphological and rheological properties of SAN/PPE blends filled with functionalized multi-walled carbon nanotubes (MWCNT) were investigated. Functionalized MWCNT with polystyrene (PS) were prepared by atom transfer radical polymerization (ATRP). Different molecular weights of grafted PS were achieved by varying the time of polymerization. MWCNT fillers were pre-mixed with SAN by solution casting. The degree of dispersion of MWCNT significantly depended on the miscibility between grafted PS and SAN. A "solid-like" behaviour at low frequencies of linear viscoelastic oscillations was observed for SAN melts filled with 2.5 wt% MWCNT. The pre-mixed SAN/MWCNT composites were blended with PPE in the melt by means of a micro-compounder. In SAN/PPE blends, pristine MWCNT with poor dispersibility stayed in the pre-mixed SAN phase. The functionalized MWCNT tended to migrate from the pre-mixed SAN phase to the PPE phase. The extent of migration depended on the molecular weight of grafted polystyrene on the surface of MWCNT. The rheological results showed that MWCNT increase the dynamic moduli G' and G'' as well as the complex viscosity of SAN/PPE blends. A higher molecular weight of grafted polystyrene effectively reduced the viscosity of PPE and thus led to a decrease of the viscosity of SAN/PPE blends filled with these functionalized MWCNT.

Keywords: SAN/PPE blends, multi-walled carbon nanotubes, rheology

*Corresponding author. Tel.: +49 4152 87 2461; fax: ++49 4152 87 2499.

E-mail address: volker.abetz@hzg.de

1. Introduction

Blending of polymers is a well-established effective and beneficial approach for providing novel materials which combine the advantageous properties of each component [1, 2]. Because of the high molecular weight and their unfavourable interaction, most polymers are immiscible so that their blends form a multiphase structure with a weak interfacial adhesion. Therefore, a large number of studies have paid attention on improving the properties of immiscible blends by means of adding a third polymeric component or fillers. In the last decade, increasing attention has focused on immiscible blends filled with carbon nanotubes (CNT), because of the excellent mechanical, electrical and thermal properties of these nanotubes [3].

In immiscible blends, the localization of CNT has a significant influence on the end-use properties. If CNT are selectively dispersed in one phase of a binary blend, the conductivity of the material can be increased at a very low CNT loading because of the phenomenon of "double percolation" [4, 5]. This phenomenon has been identified in several polymer blends, such as polyethylene/polycarbonate (PE/PC) blends [6], polycarbonate/poly(styrene-*co*-acrylonitrile) (PC/SAN) blends [7] and polyamide 6/poly (acrylonitrile-*co*-butadiene-*co*-styrene) (PA 6/ABS) blends [8]. If CNT are located at the interface of the blends, the percolation threshold can be probably achieved at the lowest CNT loading. However, this ideal localization of pristine CNT is difficult to be realized since CNT rarely have equal affinity with different components [9, 10]. Only very few kinds of functionalized CNT have been found to be massively located at the interface of immiscible blends [11, 12]. Besides, localization of CNT has an important effect on the morphology of immiscible blends. For example, if CNT are located in the matrix of blends with a droplet morphology, the viscosity of the continuous phase is increased so that the droplets of the dispersed phase can be broken up more easily [13]. In the case of co-continuous blends, Liu et al. [14] observed that functionalized CNT with a high loading can be partly located at the interface, e.g. in blends of polypropylene/poly (ethylene-*co*-vinyl) (PP/EVA) forming a "network structure". The authors pointed out that the effect combining this specific morphology of CNT and the interpenetration of two components, called "dual-net structure", is beneficial to enhance the toughness of the blends.

Poly(2,6-dimethyl-1,4-phenylene ether) (PPE) is characterized by a high heat distortion temperature, outstanding toughness and a flame-retardant behavior and has promising applications in structural parts, electronics, household and automotive items. However, the high melt viscosity of PPE leads to a poor processability even at high temperature. Thereby, modification of PPE by

means of blending with other polymers was investigated to improve the processability of neat PPE. For instance, polystyrene (PS) has been widely used to improve the properties of PPE since 1960 [15-17]. In the recent decades, poly (styrene-*co*-acrylonitrile) (SAN) has been reported as another promising candidate for blending with PPE [18-23]. Compared to polystyrene, SAN has a higher chemical resistance if the acrylonitrile (AN) content ranges between 19% and 35%. However, in this range, SAN is immiscible with PPE so that the two components form multiphase blends with a poor interfacial adhesion in the solid state. Consequently, a series of works studied the compatibilization of these immiscible blends by adding block copolymers such as poly (styrene-*b*-methyl methacrylate) (PS-*b*-PMMA) diblock copolymer [24, 25]. The polystyrene block has a thermodynamic force to enter the PPE phase [25] while the PMMA block is miscible with SAN if the AN content ranges between 20 and 35 wt% [23]. Furthermore, an improved strategy of introducing a soft rubber block was developed and intensively investigated [20-23]. Kirschnick et al. [22] reported on the melt processability of SAN/PPE blends compatibilized with polystyrene-*b*-polybutadiene-b-poly(methyl methacrylate) triblock terpolymers (SBM) by analysing the rheological and morphological properties. Ruckdäschel et al. [20, 21] systematically investigated the influence of composition and block length of SBM on the morphology and the mechanical properties of melt-processed SAN/PPE 40/60 blends. Improved mechanical properties, especially toughness, can be achieved in the case of compatibilized blends with SBM having an adequate length of PS chain [21].

Although several recent studies revealed that anisotropic nanofillers can be used as a third component to improve the morphology and properties of two-phase blends [11, 26-29], no investigation has been reported on SAN/PPE blends filled with CNT until now. In such binary blends, the localization of CNT is an important aspect which influences the end-use properties. Some previous researches suggested that surface functionalization can provide the driving force to adjust the localization of CNT resulting from the good affinity between the functionalized polymer on CNT and the blend components [10, 11, 14, 30]. Moreover, such functionalized polymers are also beneficial to improve the dispersibility of CNT in polymeric matrices [31]. In contrast to non-covalent functionalization, covalent functionalization can provide a stronger interaction between functional entities and the carbon skeleton of nanotubes [32].

In this work, SAN/PPE blends were filled with functionalized multi-walled carbon nanotubes (MWCNT). The weight ratio of SAN and PPE was 40/60, in which optimum mechanical properties were reported [21]. The functionalized MWCNT with polystyrene were prepared by “grafting from” method via atom transfer radical polymerization (ATRP). The grafted polystyrene chains on

MWCNT are expected to provide the driving force in order to tune the localization of MWCNT due to the miscibility of PS and PPE. Firstly, the functionalized MWCNT were pre-mixed with its unfavourable phase, i.e. the SAN phase. Then the pre-mixed composites were blended with PPE by extrusion. The influence of the chain length of PS on the migration of MWCNT from SAN to PPE was studied. In order to understand the relationship between structure and processing properties, the linear rheological behavior of the composites with various MWCNT was investigated in this work.

2. Experimental

2.1 Materials

Commercial poly (styrene-*co*-acrylonitrile) (SAN, Luran® 358N) was provided in granular form by BASF SE (Ludwigshafen, Germany). The content of acrylonitrile was 25 wt%. Poly (2,6-dimethyl-1,4-phenylene ether) (PPE, PX100F) powder was supplied by Mitsubishi Engineering Plastics Europe (Düsseldorf, Germany). The properties of pristine materials are listed in Table 1. Irganox 1010 and Irgafos 168 (Sigma Aldrich, Schnelldorf, Germany) were used as stabilisers for PPE at a concentration of 0.1 wt%. The ratio of Irganox 1010 to Irgafos 168 was 2.

Table 1. Properties of SAN and PPE used in this study

	Grade	Average molecular weight [a] (g/mol)		M_w / M_n	T_g [b] (°C)	η_0 [c] (Pas) (260°C)
		M_n	M_w			
SAN	Luran® 358N	83000	161000	1.95	108	900
PPE	PX 100F	12000	28000	2.42	213	45600

(a) determined by size exclusion chromatography calibrated to polystyrene

(b) determined by differential scanning calorimetry

(c) determined by rheological measurements at low frequencies

Pristine MWCNT and amino functionalized MWCNT (MWCNT-NH_2) were obtained from FutureCarbon GmbH (Bayreuth, Germany). Styrene (≥99%), 2-bromo-2-methylpropionyl bromide (2BriBr, 99%), ethy 2-bromoisobutyrate (EBiB, 99%), triethyl amine (TEA, ≥ 99.5%), copper I bromide (Cu(I)Br, 99%), N, N, N', N', N-pentamethyl diethylenetriamine (PMDETA, 97%), tetrahydrofurane (THF), chloroform (≥99%) and anisole were used as received. All the reagents were purchased from Sigma-Aldrich (Schnelldorf, Germany).

2.2 Functionalization of MWCNT with PS via ATRP

The functionalization of MWCNT followed the procedure reported by Albuerne et al. [33] and the scheme of functionalization of MWCNT is presented in Fig. 1. For anchoring initiator on MWCNT, the suspension of MWCNT-NH_2 (9.6 g) in THF (1.156 L) was immersed in an ultrasonication bath for 5 min. Then, the suspension was stirred vigorously under argon flow by using a mechanical stirrer at 120 rpm for 30 min. After this, 40 ml TEA was dropped into the system. Sequentially, the system was degassed by switching between the vacuum and argon flow for thrice. Then, the system was cooled down below 0 °C in an ice bath. A diluted solution of 2BriBr (32 ml) in THF (160 ml) was added drop-wise approximately for 1 hour. Meanwhile, the stirring speed was increased up to 700 rpm. During the whole dropping step, the reactor was covered by aluminum foil for light protection. The reaction was kept under vigorous stirring at 0 °C in the ice bath for 2 hours and subsequently at ambient temperature for 48 hours. After the reaction, the raw product was separated from mixture by filtration. In order to remove the adsorbed side products, MWCNT were washed by chloroform for several times until no blue color was observed in the filtrating liquid. Lastly, the MWCNT anchored with initiator (MWCNT-Br) was dried in an oven under vacuum at room temperature for one week.

In a typical polymerization, 2 g MWCNT-Br, 97 ml styrene (0.848 mol), 24 ml anisole (25 % v/v with respect to monomer) and 0.2 mol % of cuprous bromide (Cu(I)Br, with respect to the monomer) were dispersed in a glass flask under argon. Since it is impossible to degraft the functionalized groups form MWCNT-NH_2, 1 mol % of EBiB (with respect to the initiator on MWCNT) was added drop by drop as sacrificial initiator in order to obtain free polymers for characterization. The system was vigorously stirred by means of a magnet for 1 hour. Then, 0.2 mol % of PMDETA (with respect to the monomer) was added and the flask was transferred into an oil bath at 90 °C. In order to obtain PS chains with different molecular weights, two separate reactions with different time of polymerization (24 hours and 48 hours) were carried out under the same parameters respectively. When the reaction was completed, the mixture was diluted with THF and precipitated in methanol. The precipitated product was filtered and dried for 48 hours under vacuum. Then, the polystyrene grafted carbon nanotubes were again dispersed in THF and filtered. This procedure was repeated until no traces of polymer were collected from the filtered solution by precipitation in methanol.

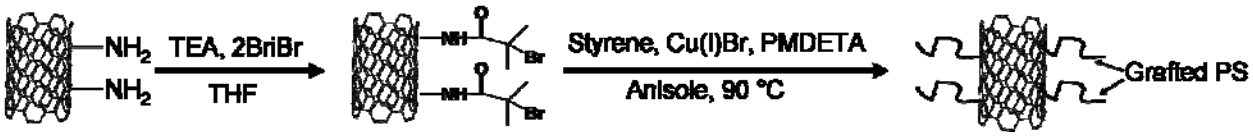

Fig. 1 Scheme of functionalization of MWCNT with polystyrene via atom transfer radical polymerization (ATRP)

2.3 Pre-mixing SAN with different MWCNT via solution casting

The preparation of the SAN/PPE blends with MWCNT was divided into two steps which are shown in Fig. 2. Firstly, MWCNT were pre-mixed with SAN using solution casting. The given amount of MWCNT was dispersed in chloroform and treated by ultrasonic probe (Bandelin SONOPULS, frequency of 20 kHz, 60 W) for 30 minutes and ultrasonic bath (Bandelin SONOREX, frequency of 35 kHz, 160 W) for 1 hour, respectively. Gel permeation chromatography was carried out in order detect a possible reduction of molecular weight caused by sonication. As the polymer cannot be degrafted from MWCNT, the free polystyrene polymerized from sacrificial initiator was treated in chloroform by ultrasoncation under the same conditions and the concentration of free polystyrene was equal to the one of grafted polystyrene in the MWCNT suspension.

Then the MWCNT suspension was mixed with a SAN solution in chloroform. The concentration of dissolved SAN was 5 wt% in chloroform. The concentration of MWCNT with respect to SAN was 2.5 wt% so that the concentration of MWCNT should be 1 wt% in the SAN/PPE 40/60 blends. After stirring vigorously for 24 hours, the suspension was directly cast in Teflon® moulds and kept on the heating plate under 40 °C for 1 day. Sequentially, the cast material was dried under vacuum at 40 °C for one more day. In order to increase the evaporating speed, the pre-mixed SAN composites with MWCNT were cut into small particles by an electrical grinder. Then, the pre-mixed particles were dried under vacuum at 80 °C for two weeks before blending with PPE.

In this work, the properties of pre-mixed SAN composites with MWCNT fillers were also investigated. The specimens for characterization were prepared by melt extrusion. The dried SAN/MWCNT particles were extruded by means of a micro-compounder with a filling volume of 15 cm^3 (DSM Xplore, Geleen, Netherlands) at 220°C. The speed of revolutions was 100 rpm and the mixing time was 5 minutes. Then, the specimens were formed by injection molding using a micro-injection moulding machine with a filling volume of 12 cm^3 (DSM Xplore, Geleen, Netherlands). The temperature in the injection chamber was 200 °C and the mould temperature was set to 100 °C. The pressure for shooting was set to 4 bar for 4 seconds. A pressure of 6 bar for 4

seconds was set for the holding process. The samples of neat SAN were prepared under the same conditions.

2.4 Preparation of SAN/PPE 40/60 blends and its composites with MWCNT

Firstly, neat SAN/PPE 40/60 blends were prepared. Prior to blending, SAN pellets and PPE powder were dried at 80 °C in a vacuum for at least 12 hours. The components were melt-blended in a micro-compounder with a filling volume of 15 cm^3 (DSM Xplore, Geleen, Netherlands) at 300 °C. The speed of revolutions was 100 rpm and the mixing time was 5 minutes.

The specimens for morphological and rheological measurements were prepared by using a micro-injection moulding machine with a filling volume of 12 cm^3 (DSM Xplore, Geleen, Netherlands). The temperature in the injection chamber was 280 °C and the mould temperature was set to 100 °C. The pressure for shooting was set to 4 bar for 4 seconds. A pressure of 6 bar for 4 seconds was set for the holding process.

Melt blending of SAN/PPE composites with MWCNT was performed in a similar way as for the neat blend described above. The only difference was using the dried SAN/MWCNT powder instead of neat SAN pellets during processing. The samples of neat PPE were prepared under the same processing conditions as the procedure for the SAN/PPE blends.

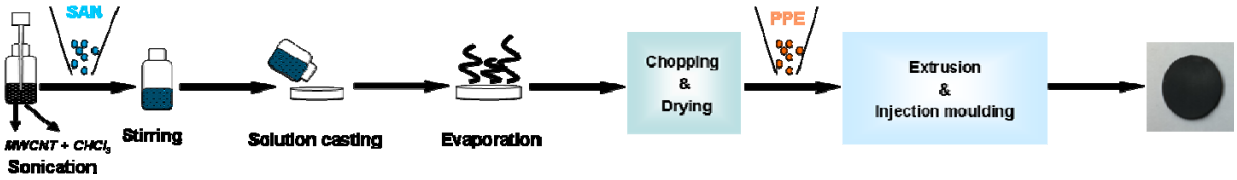

Fig. 2 Scheme of preparation of SAN/PPE 40/60 blends filled with MWCNT

2.5 Characterization

2.5.1 Differential scanning calorimetry

The glass transition temperature T_g of SAN and PPE was measured by differential scanning calorimetry (DSC) using a Netzsch DSC Phoenix. The equipment was calibrated using indium and cyclohexane. Standard aluminum pans of 50 µl were used to encapsulate the sample. The mass of the samples was approximately 10 mg. The samples were first heated up to 250 °C, cooled down to 25 °C, and heated up again to 250 °C for the second circle. All measurements were done under nitrogen atmosphere at a constant heating and cooling rate of 10 °C/min. The T_g value was determined based on the data of the second heating cycle.

2.5.2 Gel permeation chromatography and thermal gravimetric analysis

The average molecular weight of the neat polymer components and the free PS polymerized from sacrificial initiator was characterized by gel permeation chromatography (GPC) and analysis by an UV detector using THF as a solvent and standard polystyrene (PS) as calibration.
Thermal gravimetric analysis (TGA) was carried out using a TGA device Netzsch TG209 F1 Iris. The measurement was conducted at constant argon flow with a flow rate of 20 ml/min. The temperature range was 25 °C to 1000 °C, and the heating rate was 10 °C/min.

2.5.3 Fourier transform infrared spectra

The functionalized MWCNT were detected by Fourier transform infrared spectra (FT-IR) using Bruker Equinox 55. The samples were carefully dispersed in potassium bromide (KBr) and then placed in a vacuum oven at 60°C for 24 hours. The content of carbon nanotubes in KBr pellets was 0.1 wt% in the case of pristine MWCNT and 0.5 wt% in the case of PS-grafted MWCNT. The infrared spectra were recorded in a spectral range of 800- 3200 cm^{-1} with a spectral resolution of 1 cm^{-1}.

2.5.4 Transmission and scanning electron microscopy

Transmission electron micrographs (TEM) were taken with a Tecnai F20 (FEI) operated at 200kV in bright field mode. Ultrathin sections of approx. 50 nm were obtained at room temperature of a disc prepared for rheological experiments by a Ultramicrotome (Leica) equipped with a diamond knife.

Scanning electron microscopy (SEM) was utilized to determine the miscibility of SAN and grafted PS with high molecular weight. The experiment was carried out with a LEO Gemini 1550VP from Zeiss. The extruded sample was broken under liquid nitrogen condition. Then the sample was sputtered with a Pt layer with a thickness of 1.5 nm for analysis of the cross section.

2.5.5 Rheological measurement

The rheological properties of the pristine blend components and the blends were analyzed using the rotational rheometer ARES (Rheometrics Scientific, Piscataway, USA) in parallel-plates configuration. The diameter of the samples was 20 mm and the gap was 1.6 mm. In order to minimize thermal degradation, all measurements were performed in a nitrogen atmosphere. The temperature for all tests was 260 °C. The time for annealing the samples was 8 minutes before each test. The thermal stability was characterized by dynamic time sweeps at an angular frequency ω of

0.5 rad/s and a strain amplitude γ_0 of 10%. The storage and loss modulus were measured as a function of angular frequency in a range of 0.01-100 rad/s starting at the largest frequency. Prior to these measurements, dynamic strain sweeps were carried out in the range of 1-10% at an angular frequency of 10 rad/s in order to determine the linear viscoelastic region.

3. Results and discussion

3.1 Thermal properties of PS-grafted-MWCNT

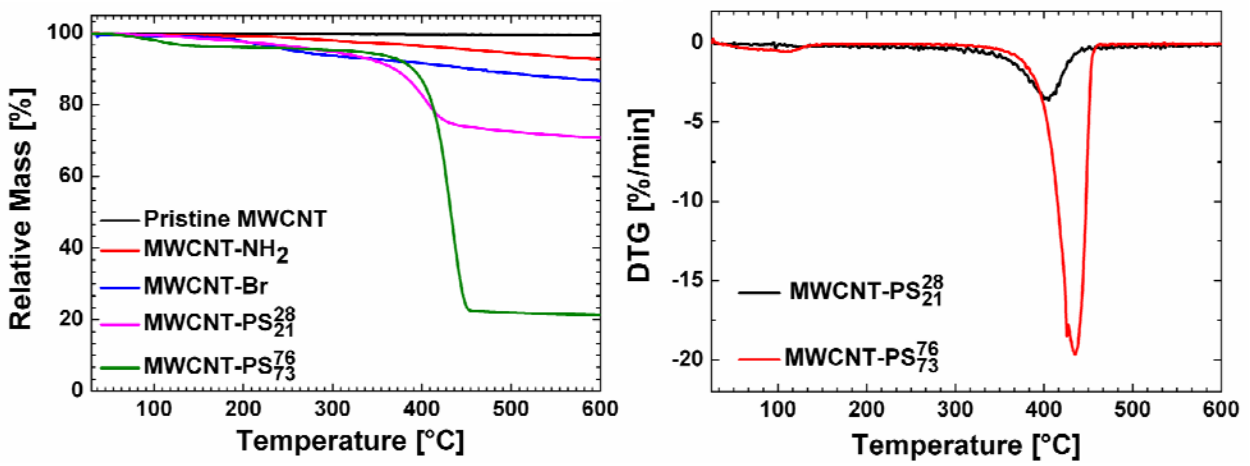

(a) (b)

Fig. 3 Results of TGA measurements of pristine MWCNT and functionalized MWCNT (a) and DTG measurements of functionalized MWCNT (b). The heating rate was 10 K/min and a nitrogen atmosphere was applied.

The molecular weight of grafted PS on MWCNT was detected by GPC using the free polystyrene polymerized from sacrificial initiator. In order to analyze the influence of the ultrasonication procedure on the molecular weight of polystyrene, the molecular weight of free PS after sonication was also characterized and summarized in Table 2. The data indicates that the ultrasonication procedure has only a slight effect on the molecular mass of grafted PS on the surface of MWCNT. This phenomenon can be explained by the relative low molecular weight of grafted PS and is in accordance with previous research on the effect of ultrasonication on the molecular weight of PS in toluene [34].

In order to determine the PS content of functionalized MWCNT, TGA measurements were performed. As shown in Fig. 3, the as-received pristine MWCNT exhibit an excellent thermal stability with a weight loss of less than 1 wt% above 100 °C. The curves of MWCNT-NH_2 and MWCNT-Br gradually decrease with temperature. As revealed by the derivative of the thermogravimetry (DTG) curve, the peaks of the DTG curves are located between 330 °C and 470

°C. The relative mass is approximately constant above 500 °C. Thus, the mass loss is determined by the data in the temperature range from 100 °C to 550 °C for each sample. Furthermore, in the case of pristine MWCNT, the weight loss slightly increased and no pronounced and clear characteristic peak could be seen in the DTG curve. Therefore, we only present the DTG of functionalized MWCNT with polystyrene in Fig. 3(b).

With respect to the functionalized MWCNT, the received MWCNT-NH_2 show a weight loss of 5.9 wt% corresponding to a concentration of amino groups of 6.4 mmol/g on the surface of MWCNT. After the anchoring process, 0.379 mmol/g (11.6 wt%) initiator was successfully bound to the MWCNT. For the functionalized MWCNT with a low molecular weight of PS (21,000 g/mol), the content of grafted polymer was 28 wt% with respect to the total weight of functionalized MWCNT. For a molecular weight of grafted PS of 73,000 g/mol, the content increased to 76 wt%. In the following discussion, the content of PS is denoted by superscripts, and the molecular weight of PS is shown by subscripts. Considering the density of grafted PS on the surface of the nanotubes cannot be precisely determined, we compared the ratio of the mass loss versus the molecular weight in order to detect the relative density of PS on the MWCNT for these two functionalized MWCNT. Since the concentrations of the initiator on these MWCNT are constant, the densities of grafted PS of these two kinds of modified MWCNT should be equal which implies that the mass loss of PS groups should proportionally increase with molecular weight. In the case of MWCNT-$PS^{28}_{21,}$ the ratio is $1.30*10^{-5}$, and the corresponding value of MWCNT-PS^{76}_{73} is $1.04*10^{-5}$. These values reveal that the functionalized MWCNT with a higher molecular weight of PS have a lower density of PS. This result can be explained by the fact that, the long polymer chains of high molecular weight PS wind with each other on the surface of MWCNT so that the further growth of relatively short chains might be blocked during propagation. Nevertheless, this difference due to the approach of functionalization is very slight and unavoidable. Thereby, in our following discussion, the densities of PS for these two functionalized MWCNT are assumed to be equal. The properties of functionalized MWCNT with PS are listed in Table 2.

Table 2. Summary of functionalized MWCNT with PS

Codes	[Br] (a) (mmol/g)	Time (hours)	Weight loss(a) (wt%)	M_n (b) (g/mol)	PDI	Weight loss/ M_n (wt%/(g/mol))	After sonication	
							M_n (b) (g/mol)	PDI
MWCNT-PS^{28}_{21}	0.379	24	28	21,000	1.08	$1.30 * 10^{-5}$	20,000	1.09
MWCNT-PS^{76}_{73}	0.379	48	76	73,000	1.13	$1.04 * 10^{-5}$	73,000	1.13

(a) determined by thermal gravimetric analysis

(b) determined by size exclusion chromatography calibrated to polystyrene

3.2 FT-IR analysis of functionalized MWCNT

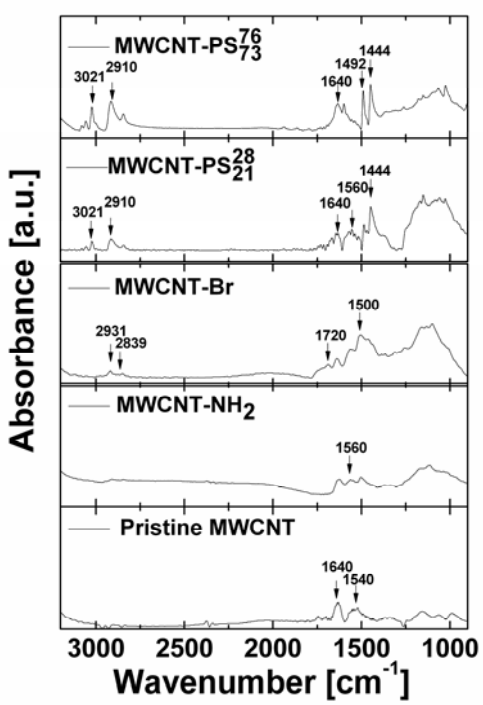

Fig. 4 FT-IR spectra of pristine MWCNT and different functionalized MWCNT.

FT-IR spectra of pristine MWCNT and functionalized MWCNT are presented in Fig. 4. Compared to pristine MWCNT, the typical signals for aromatic systems (900-1200 cm^{-1}) are detected in all spectra of the functionalized MWCNT samples, which results from the covalent functionalization on the surface of the tubes [35]. In previous studies, the signal between 1650 cm^{-1} and 1540 cm^{-1} were attributed to the C=C stretching mode of aromatic ring [33, 36, 37]. Compared to pristine MWCNT, an additional peak locating at 1560 cm^{-1} corresponding to the amine group is observed in the spectra of MWCNT-NH_2 [38]. After anchoring the initiator, the -CH stretching peaks from

alkyl chains at 2931 cm^{-1} ~ 2839 cm^{-1} and the –C=O stretching peak from the ester linkage at 1720 cm^{-1} appear, which reveal the presence of a 2BriB group on the surface of MWCNT [39]. In the two kinds of functionalized MWCNT with polymer, the PS component is determined by the characteristic peaks at 3100-2800 cm^{-1} corresponding to the stretching vibration of C-H, the signals at 1500-1638 cm^{-1} resulting from the unsaturation sites in the benzene ring as well as the peaks at 1492 cm^{-1} and 1444 cm^{-1} attributing to both of stretching vibration of aromatic ring and the deformation vibration of $–CH_2$ [33]. Furthermore, a broad peak locating at 1560 cm^{-1} was found in the spectra of MWCNT-PS^{28}_{21}. This phenomenon can be explained by the overlapped the signals resulting from both MWCNT and PS, as the signals from MWCNT between 900-1200 cm^{-1} are also strong in case of MWCNT-PS^{28}_{21}. On the other hand, in case of MWCNT-PS^{76}_{73}, the content of PS is 76 wt% so that the characteristic peaks of polystyrene are strongly pronounced and the signals from MWCNT became weak. From the FT-IR spectra, we can conclude that the MWCNT were successfully functionalized.

3.3 Morphology of SAN/PPE 40/60 blends and its composites with different MWCNT

3.3.1 SAN/MWCNT composites

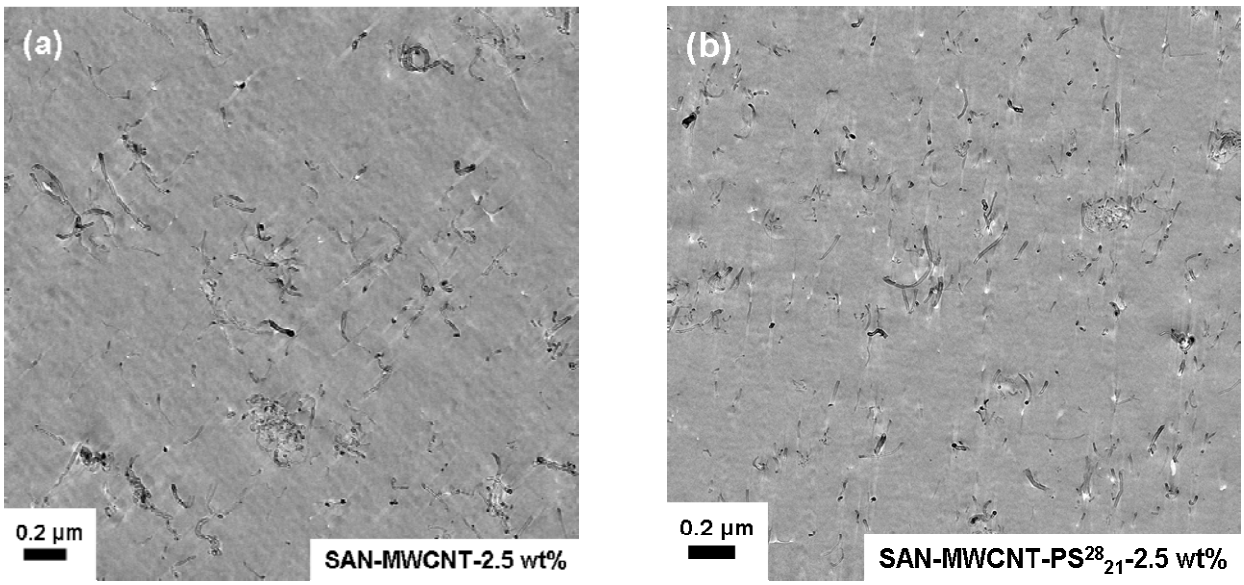

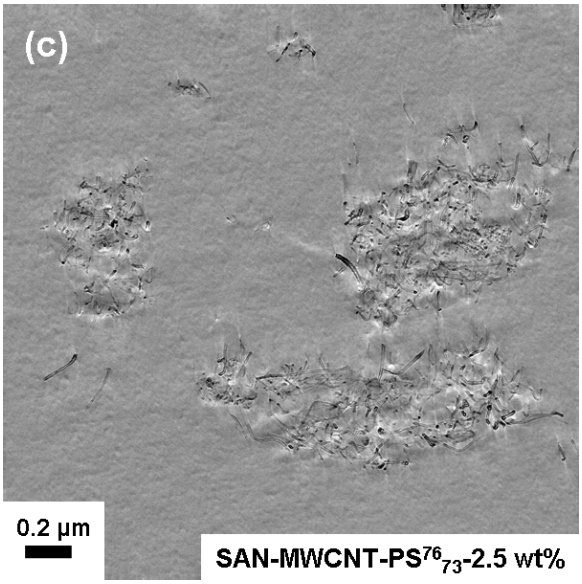

Fig. 5 TEM micrographs of SAN composites with various MWCNT fillers:
(a) SAN composites with pristine MWCNT (2.5 wt%); (b) SAN composites with MWCNT-PS$^{28}_{21}$ (2.5 wt%); (c) SAN composites with MWCNT-PS$^{76}_{73}$ (2.5 wt%).

The dispersion of MWCNT fillers in SAN was analyzed by TEM. The objective was to study the influence of functionalized PS on the dispersibility of MWCNT in SAN. The micrographs showed stripes from the cutting direction of the diamond knife. These stripes were removed by eliminating the respective signals in the Fourier Transform of the image and then back transforming to the filtered image following a procedure described by Michler [40]. The original images can be found in the section of experimental supporting materials. As shown in Fig. 5(a), a large fraction of pristine MWCNT is agglomerated and a minor fraction of MWCNT is well dispersed in the matrix due to the ultrasonication treatment. In contrast, MWCNT-PS$^{28}_{21}$ present a better dispersibility than the pristine ones. Interestingly, if the molecular weight of grafted PS increases, the functionalized MWCNT tend to aggregate again, as seen in Fig. 5(c). Furthermore, the agglomerates of MWCNT-PS$^{76}_{73}$ are more equally sized than the inhomogeneous aggregates of pristine MWCNT. These different degrees of dispersion of functionalized MWCNT in SAN can be explained by the miscibility between SAN and grafted PS which varies with the molecular weight of PS. Since the T_g of SAN and PS do not differ much, we determined the miscibility of SAN and grafted PS with high molecular weight by scanning electron micrographs (SEM). The free PS polymerized from sacrificial initiator were blended with SAN by extrusion under the same condition of preparing the composites with MWCNT. The ratio of SAN to PS in the SAN/PS blend was 92 to 8 which is equal to the composition of SAN composites with functionalized MWCNT. In Fig. 6, the micrographs of

blends of SAN and free PS revealed that PS and SAN formed a two-phase blend for the high molecular weight polystyrene. A similar effect was reported by Haase et al.[41].

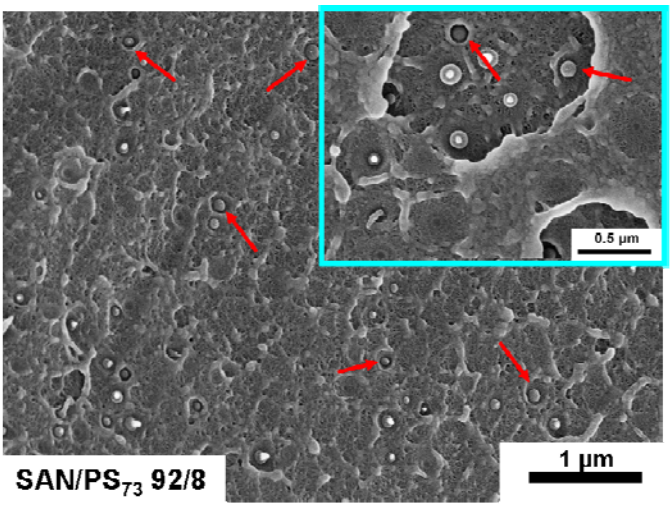

Fig. 6 SEM micrograph of SAN/PS_{73} 92/8 blends. The arrows indicate the PS drops in the SAN matrix.

3.3.2 SAN/PPE blends and its composites

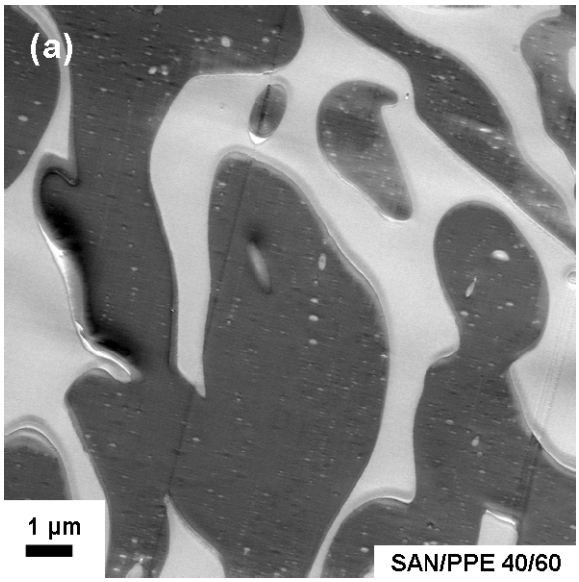

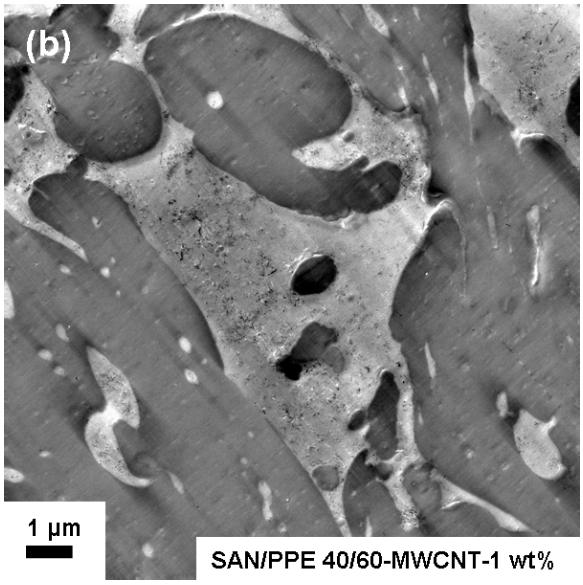
(b)
1 µm
SAN/PPE 40/60-MWCNT-1 wt%

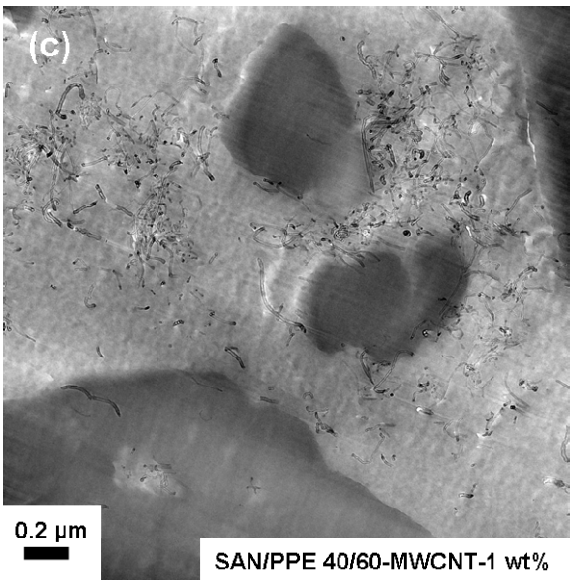
(c)
0.2 µm
SAN/PPE 40/60-MWCNT-1 wt%

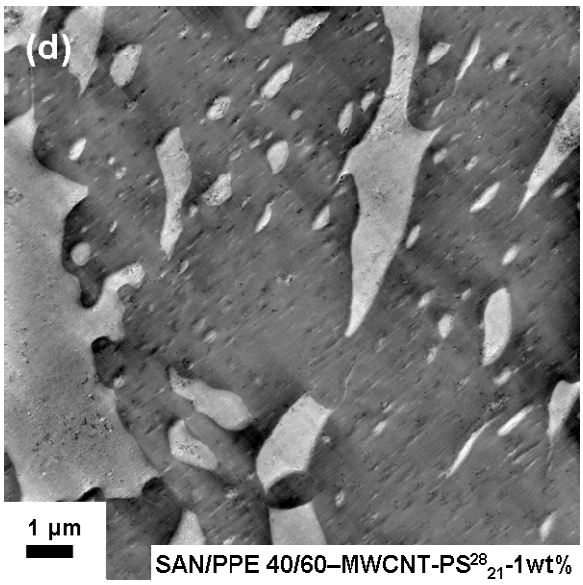
(d)
1 µm
SAN/PPE 40/60–MWCNT-PS$^{28}_{21}$-1wt%

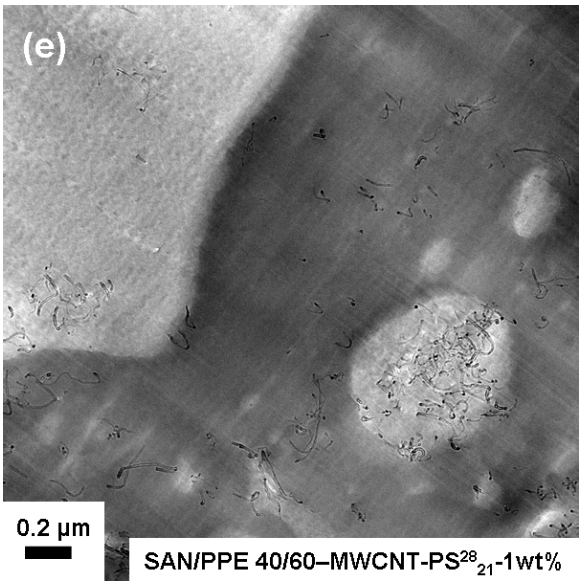
(e)
0.2 µm
SAN/PPE 40/60–MWCNT-PS$^{28}_{21}$-1wt%

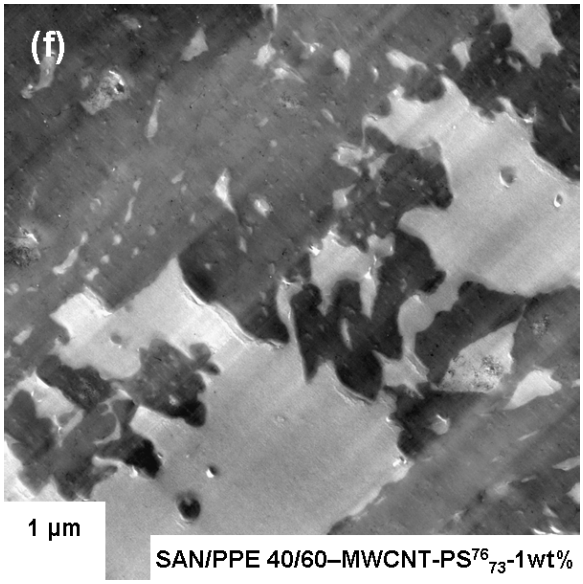
(f)
1 µm
SAN/PPE 40/60–MWCNT-PS$^{76}_{73}$-1wt%

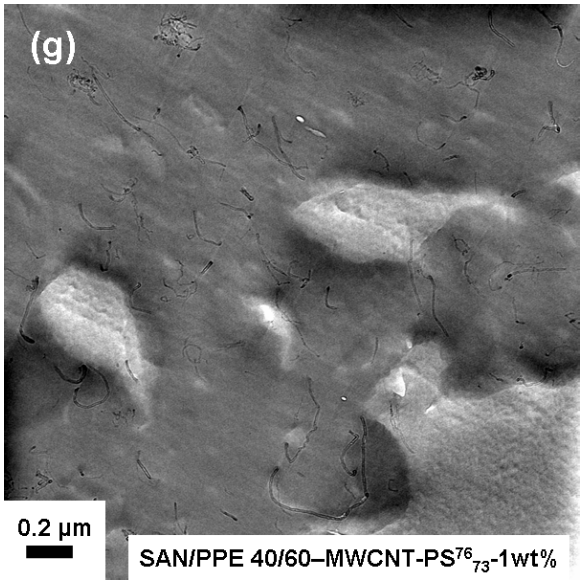
(g)
0.2 µm
SAN/PPE 40/60–MWCNT-PS$^{76}_{73}$-1wt%

Fig. 7 TEM micrographs of SAN/PPE 40/60 blends and its composites with various MWCNT having different surface functionalization: (a) SAN/PPE 40/60; (b-c) SAN/PPE-MWCNT-1 wt%; (d-e) SAN/PPE-MWCNT-PS^{28}_{21}-1 wt%; (f-g) SAN/PPE-MWCNT-PS^{76}_{73}.

TEM micrographs of SAN/PPE blend and its composites filled by MWCNT are shown in Fig. 7. In the micrographs, the PPE phase appears in black and the bright phase corresponds to SAN. The morphology of neat SAN/PPE 40/60 blends is shown in Fig. 7(a). Although a co-continuous structure is not achieved, the dispersed PPE phase does not form droplets but a structure with a certain continuity. As known from the previous work of Ruckdäschel et al., SAN/PPE 40/60 with such structure appear most promising because of its a remarkably toughness, a satisfying processability and enhanced thermo-mechanical properties [20].

For the composites based on SAN/PPE blends, the localization of MWCNT in the blends plays an important role. Like the micrographs in Fig. 5, the images of composites with MWCNT (from Fig. 7(b) to Fig. 7(g)) were also filtered by Fourier Transform method [40] and the original images were presented in the supporting information. Despite of a tiny size of dispersed MWCNT, the presence of nanofillers can be distinguished by the colour change of the brighter SAN phase. As shown in Fig. 7(b), the SAN phase becomes more grey and ruffed compared to the neat blends, indicating a presence of large amount of MWCNT in the SAN phase even after extrusion. Most of MWCNT are aggregated. In Fig. 7(c) with high magnification, only very few isolated MWCNT are located in the PPE phase. The localization of MWCNT in immiscible blends is influenced by both the affinity of polymer to MWCNT fillers and the viscosity of the polymeric components. In immiscible blends, MWCNT tend to be located in the polymer phase with a higher affinity to them or a lower viscosity [42]. In SAN/PPE blends, localization of MWCNT in the PPE phase which has a dramatically higher viscosity than SAN indicates that PPE exhibit a larger thermodynamic affinity to MWCNT than SAN. However, the tendency is not strong enough to induce a large fraction of MWCNT to migrate, especially for the aggregated MWCNT which need high driving force to disperse and move.

After functionalization with polystyrene, a large amount of MWCNT migrates into the PPE phase (Fig. 7(d) and (e)). In contrast to the morphology of SAN/PPE-MWCNT composite, the grey regions of the SAN phase in SAN/PPE 40/60-MWCNT-PS^{28}_{21} become brighter indicating a decreasing amount of MWCNT fillers. In Fig. 7(e), well dispersed MWCNT are selectively located in the PPE phase. As the surface of functionalized MWCNT is already covered by the grafted PS, the migration of MWCNT fillers can contribute to the good thermodynamic miscibility of PPE and PS with any composition. However, in this composite, the low molecular weight of PS grafted on MWCNT correspond to a relative thin polymeric layer, so that, the driving force is not sufficient

for a high degree of migration. Hence, some aggregated bundles still remain inside the SAN phase (Fig. 7(e)).

However, a strong driving force can be obtained in the case of MWCNT-PS$^{76}_{73}$ resulting from the increasing PS content. As shown in Fig. 7(f) and (g), almost all functionalized MWCNT are located in the PPE phase in the case of the composites with MWCNT-PS$^{76}_{73}$. The SAN phase in this composite displays as bright as the one in the neat blend and few MWCNT can be observed in this region. As discussed above, MWCNT-PS$^{76}_{73}$ exhibit a poor dispersibility in the SAN matrix because of the immiscibility (Fig. 6). After blending with PPE, the migrated MWCNT present a good dispersion with a large fraction of isolated MWCNT locating in PPE (Fig. 7(g)). This phenomenon is in agreement with the beneficial effect of grafting groups on the dispersibility of nanotubes.

3.4 Rheological properties

3.4.1 Thermal stability of neat SAN and PPE

In order to detect the thermal stability of the neat blend components during the measurements, dynamic time sweep tests were carried out at a low frequency (ω = 0.5 rad/s). The time for the measurements was 5000 s which is long enough to grant a sufficient stability for the frequency sweep.

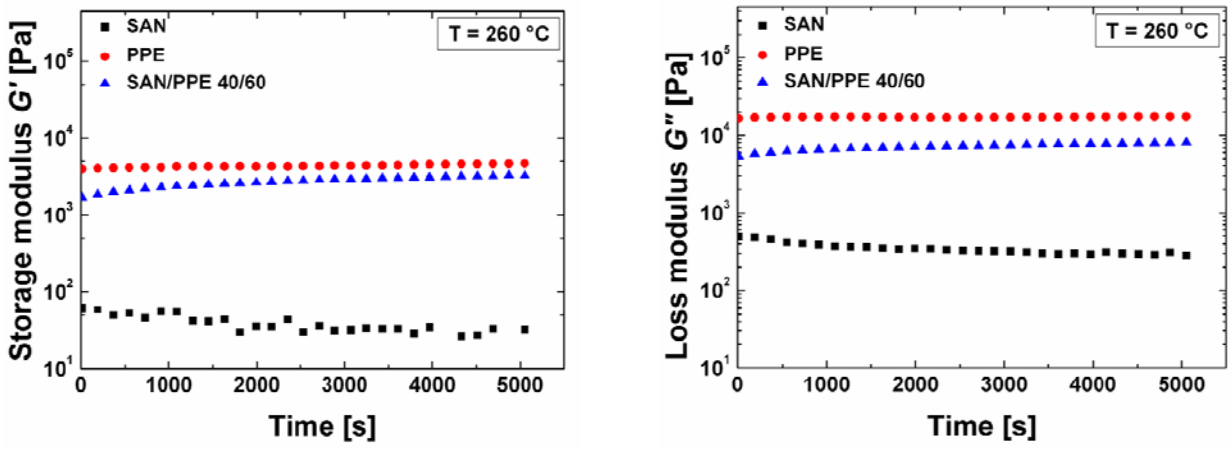

(a) (b)

Fig. 8 Storage modulus G' (a), loss modulus G'' (b) of SAN and PPE as a function of time at 260 °C.

The constant values of G' and G'' in Fig. 8 indicate a good stability of SAN and PPE during the whole time of measurement. The scattering of G' of SAN results from the resolution of the device. Moreover, the molecular weights of the polymers before and after measurement of the raw materials are listed in Table 3. The molecular weight of PPE significantly increases after melt

processing. This phenomenon is in agreement with previous investigation [43] and can be explained by the further chain growth originating from the ending hydroxyl group of PPE at the high processing temperature.

Table 3. Summary of molecular weight (g/mol) of SAN and PPE at different processing steps (as determined by size exclusion chromatography calibrated to polystyrene)

	Raw material			After melt processing			After the measurement		
	M_w	M_n	M_w/M_n	M_w	M_n	M_w/M_n	M_w	M_n	M_w/M_n
SAN	161000	83000	1.95	138000	53000	2.61	149000	68000	2.21
PPE	28000	12000	2.42	40000	18000	2.19	46000	19000	2.44

3.4.2 Linear viscoelastic properties of neat SAN and pre-mixed SAN composites with MWCNT

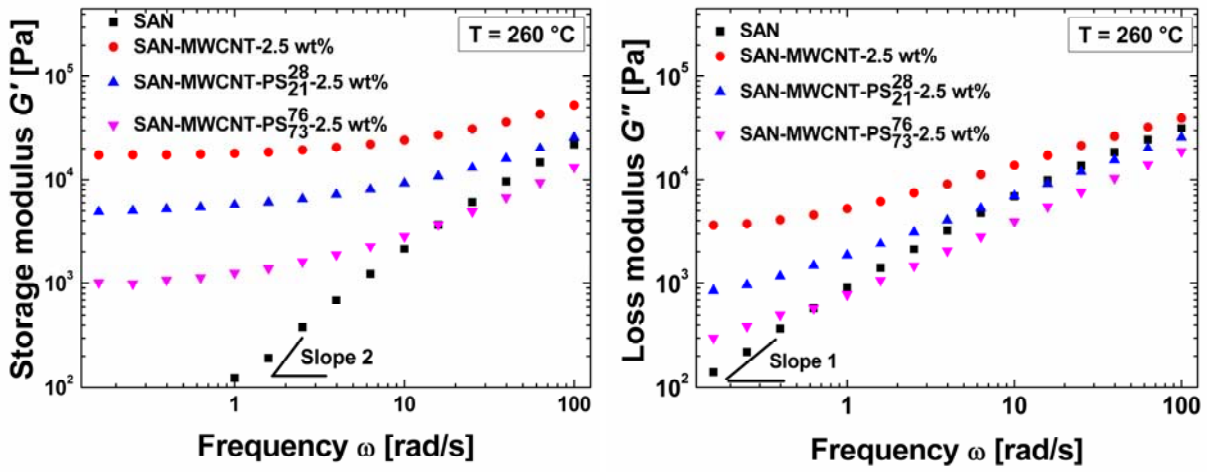

(a) (b)

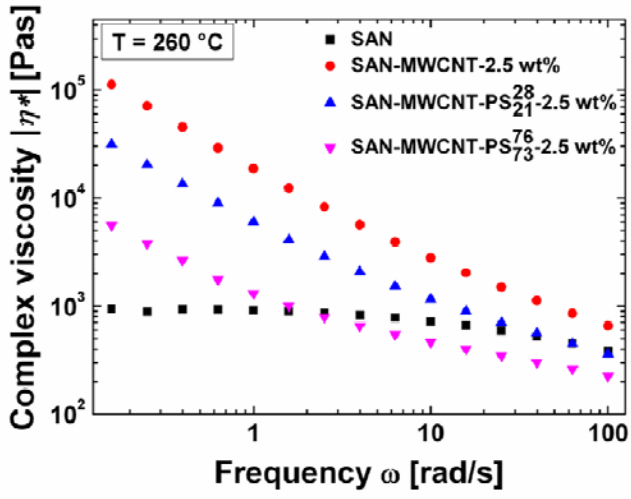

(c)

Fig. 9 Storage modulus G'(a), loss modulus G''(b) and complex viscosity $|\eta^*|$ (c) of SAN and its pre-mixed SAN/MWCNT composite as a function of angular frequency at 260°C.

The rheological properties of neat SAN and its composites with various MWCNT fillers are presented in Fig. 9. For neat SAN, the storage and the loss modulus increase with angular

frequency ω and exhibit a typical terminal behavior at low frequencies, revealing a full relaxation of SAN chains. After addition of MWCNT fillers, the terminal behavior disappears and the dependence of G' and G'' on angular frequency ω becomes weak. This remarkable non-terminal behavior attributes to the fact that CNT-CNT interactions start to dominate because of the relatively high MWCNT concentration (2.5 wt%). Similar plateaus of G' and G'' versus frequency at low frequencies were also observed and extensively investigated in other polymer composites with MWCNT [44, 45]. Besides, the complex viscosity of SAN and its composites are in accordance with the transition from a liquid-like to a solid-like behavior. As shown in Fig. 9(c), the neat SAN displays a typical Newtonian plateau within the measured frequency range, whereas the composites with MWCNT exhibit a strong shear thinning effect.

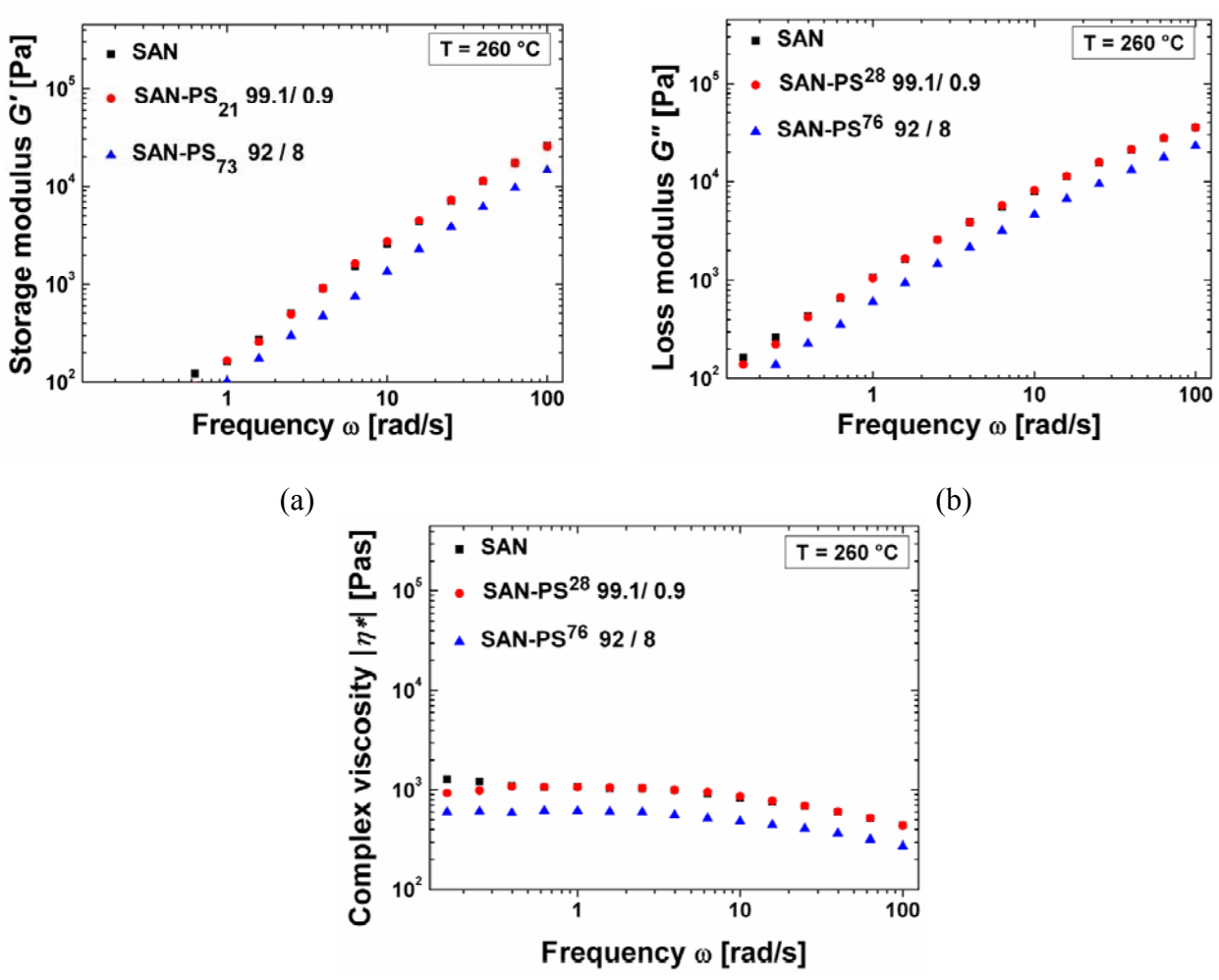

Fig. 10 Storage modulus G'(a), loss modulus G''(b) and complex viscosity $|\eta^*|$ (c) of SAN/PS blends, as a function of angular frequency at 260°C.

Interestingly, the dynamic moduli and the complex viscosity of the composites with functionalized MWCNT are lower than the ones with pristine MWCNT. The reduction of the dynamic moduli and

complex viscosity most probably are caused by the grafted PS, which has a relatively low viscosity. Since the content of grafted PS increases with molecular weight, the decrease of G' and G'' is mostly pronounced in the case of SAN-MWCNT-PS^{76}_{73}. As we observed in the TEM micrographs, a high content of immiscible PS leads to agglomeration of MWCNT. Thus, the dynamic moduli and complex viscosity of this composite are lower than the properties of neat SAN at high frequencies, revealing a similar behavior to SAN/PS blends. In order to determine the effect of PS, the rheological properties of SAN/PS was carried out as shown in Fig. 10. The PS component is the free polymers synthesized from the sacrificial initiator. The composition of these SAN/PS blends is equal to the composition of SAN composites with functionalized MWCNT with PS. Hence, the comparison with the neat SAN shows the softening effect of high molecular weight PS because of the lower dynamic moduli and the complex viscosity of $SAN\text{-}PS_{73}$ 92/8.

3.4.3 *Linear viscoelastic properties of SAN/PPE 40/60 composites with various MWCNT*

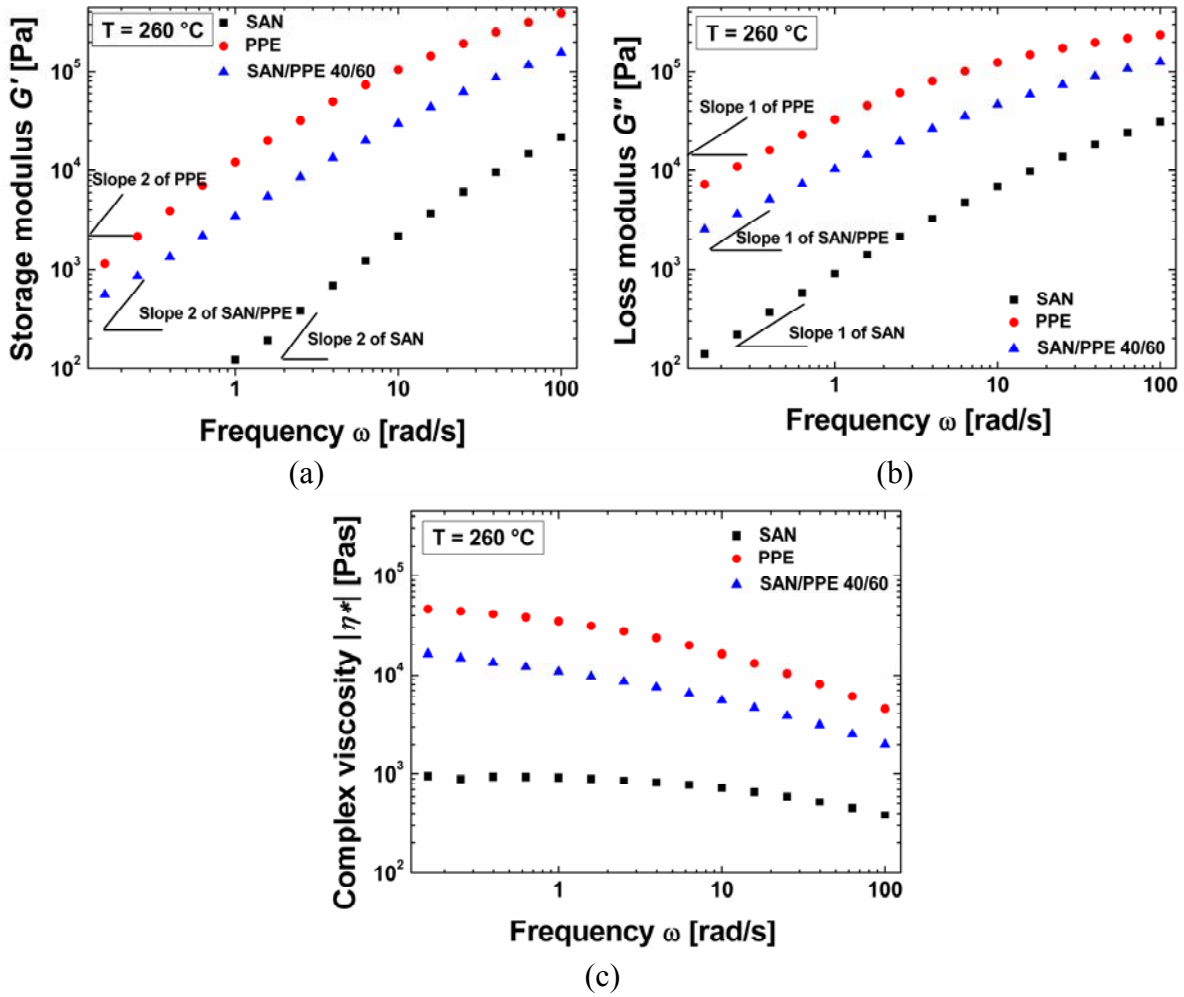

Fig. 11 Storage modulus G'(a), loss modulus G''(b) and complex viscosity $|\eta^*|$ (c) of neat SAN, PPE and SAN/PPE 40/60 as a function of angular frequency at 260°C.

Firstly, the rheological properties of neat SAN/PPE blends are discussed. In Fig. 11, SAN and PPE perform a typical terminal behaviour with the scaling relations $G' \propto \omega^2$ and $G'' \propto \omega$, indicating the full relaxation of these polymers. The slope of G' of SAN/PPE 40/60 blends at low frequencies is smaller than 2. This behaviour is caused by the presence of interfacial tension between the two immiscible phases [46, 47].

The rheological properties of SAN/PPE composites with MWCNT fillers are presented in Fig. 12. The results of the neat blends are also shown for comparison. Because of their anisotropic shape and their flexibility, the presence of MWCNT enhances the moduli and complex viscosity of SAN/PPE blends. The terminal behaviour of the neat blends disappears due to the addition of MWCNT. Meanwhile, the complex viscosity of the blends also increases by addition of MWCNT. A decrease of complex viscosity with angular frequency can be seen in the plots. However, as the content of MWCNT in SAN/PPE blends is lower than the one in SAN/MWCNT composites, the effect of MWCNT in the blends is not as pronounced as the one in the SAN matrix.

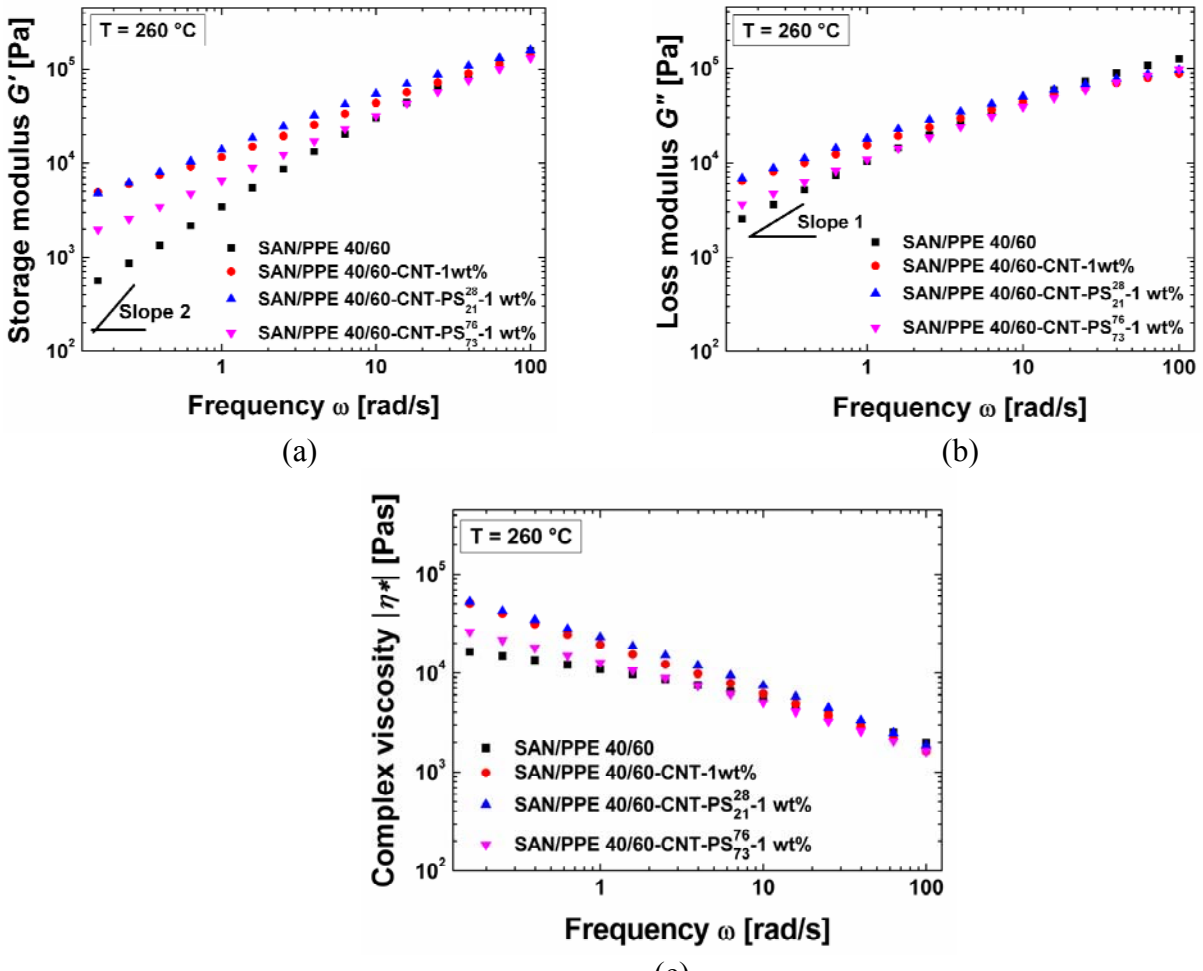

Fig. 12 Storage modulus G' (a), loss modulus G'' (b) and complex viscosity $|\eta^*|$ (c) of SAN/PPE 40/60 and its composites with different MWCNT fillers as a function of angular frequency at 260 °C.

Functionalized MWCNT with PS are expected not only to enhance the dispersibility of nanofillers, but also to improve the processability of PPE. Therefore, the influence of grafted PS on the rheological properties of MWCNT in SAN/PPE 40/60 blends attracted our interest. In contrast to the composites with pristine MWCNT, the dynamic moduli and the complex viscosity of SAN/PPE 40/60-MWCNT-PS^{76}_{73} composites dramatically decreased. The TEM micrographs (Fig. 7) indicate that these functionalized MWCNT are mainly located in the PPE phase. Hence, the decreased values of SAN/PPE composites with functionalized MWCNT should contribute to the change of the PPE phase which is softened by grafted PS [48]. The composite of SAN/PPE 40/60-MWCNT-PS^{28}_{21} performs a quite similar behaviour to the material with pristine MWCNT, although the morphologies of the two composites are different. Since MWCNT are located in both of the SAN and PPE phase, for this composite with a low molecular weight of PS, the content of MWCNT for each component is very low so that the effect of grafted PS is not pronounced due to the low loading. Furthermore, the low molecular weight of grafted PS results in a low concentration of PS. In the case of MWCNT-PS^{76}_{73}, the content of PS is 3 wt% with respect to the weight of the composites, while, the corresponding value of MWCNT–PS^{28}_{21} is only 0.4 wt%. Thus, no remarkable influence on the rheological properties can be achieved if SAN/PPE blends are filled with MWCNT-PS^{28}_{21}. In conclusion, the rheological properties of SAN/PPE composites with functionalized MWCNT are influenced by the combined effect of grafted PS in the blends and the location of MWCNT.

4. Conclusions

SAN/PPE composites with various MWCNT were prepared by melt processing. Prior to melt blending, all kinds of MWCNT nanofillers were pre-mixed with SAN via solution casting. Compared to neat SAN, the composites filled with MWCNT presented a pronounced “solid-like” behavior due to the high loading of fillers (2.5 wt%). The dynamic moduli of G' and G'' as well as the complex viscosity of SAN decreased with increasing content of PS on MWCNT due to the influence of PS.

SAN/PPE 40/60 composites filled with 1 wt% of MWCNT were prepared by blending with PPE. In the blends, pristine MWCNT stayed in the pre-mixed SAN phase whereas the functionalized MWCNT tended to migrate to the PPE phase driven by the miscibility between PPE and grafted PS on the surface of MWCNT. Furthermore, the extent of migration strongly depended on the molecular weight of polystyrene in MWCNT fillers. In addition, rheological properties reflected the

effect of both the content of polystyrene and the location of MWCNT. When functionalized MWCNT contain a high molecular weight of polystyrene (73,000 g/mol), most of the nanofillers migrated into the PPE phase leading to a decrease of both dynamic moduli and complex viscosity. Functionalized MWCNT with a lower molecular weight PS (21,000 g/mol) presented a similar rheological behavior which is similar to the one of pristine MWCNT because of the low density of MWCNT in each component and the low concentration of PS in the blends (0.4 wt%).

Acknowledgement

The authors are grateful to Clarissa Abetz for carrying out TEM and Anne Schroeder for SEM investigation, Silvio Neumann for DSC measurements, Heinrich Böttcher, Ivonne Ternes and Berthold Wendland for experimental support. The authors also thank BASF SE (Ludwigshafen, Germany) and FutureCarbon GmbH (Bayreuth, Germany) for supplying SAN and MWCNT, respectively. This work was financially supported by the 7th Framework Program research EU-project "HARCANA" (Grant Agreement No: NMP3-LA-2008-213277).

References

1. Utracki LA. Polymer Alloys and Blends: Thermodynamics and Rheology. München: Hanser Publisher, 1989.
2. Paul DR. Polymer blends. New York: Academic Press, 1978.
3. Iijima S. Nature 1991;354(7):56-58.
4. Baughman RH, Zakhidov AA, and Heer WA. Science 2002;297(5582):787-792.
5. Meincke O, Kaempfer D, Weickmann H, Friedrich C, Vathauer M, and Warth H. Polymer 2004;45(3):739-748.
6. Pötschke P, Bhattacharyya AR, and Janke A. Polymer 2003;44(26):8061-8069.
7. Göldel A, Kasaliwal G, and Pötschke P. Macromolecular Rapid Communications 2009;30(6):423-429.
8. Lee GW, Jagannathan S, Chae HG, Minus ML, and Kumar S. Polymer 2007;49(7):1831-1840.
9. Baudouin AC, Bailly C, and Devaux J. Polymer Degradation and Stability 2010;95(3):389-398.
10. Tao FF, Nysten B, Baudouin AC, Thomassin JM, Vuluga D, Detrembleur C, and Bailly C. Polymer 2011;52(21):4798-4805.
11. Wu DF, Wu LF, Zhang M, Zhou WD, and Zhang YS. Journal of Polymer Science Part B: Polymer Physics 2008;46(12):1265-1279.
12. Bose S, Bhattacharyya AR, Khare RA, Kulkarni AR, and Pötschke P. Macromolecular Symposia 2008;263(1):11-20.
13. Liu XQ, Yang W, Xie BH, and Yang MB. Materials & Design 2011;34:355-362.
14. Liu L, Wang Y, Li YL, Wu J, Zhou ZW, and Jiang CX. Polymer 2009;50(14):3072-3078.
15. Stoelting J, Karasz FE, and Macknight WJ. Polymer Engineering & Science 1970;10(3):133-138.
16. Cavaille J, Etienne S, and Perez J. Polymer 1986;27(4):549-562.
17. Utracki LA. Polymer Engineering & Science 1982;22(17):1166-1175.

18. Merfeld GD, Karim A, Majumdar B, Satija SK, and Paul DR. Journal of Polymer Science Part B: Polymer Physics 1998;36(37):3115-3125.
19. Lach R, Grellmann W, Weidisch R, Altstädt V, Kirschnick T, Ott H, Stadler R, and Mehler C. Journal of Applied Polymer Science 2000;78(11):2037-2045.
20. Ruckdäschel H, Sandler JKW, Altstädt V, Rettig C, Schmalz H, Abetz V, and Müller AHE. Polymer 2006;47(8):2772-2790.
21. Ruckdäschel H, Sandler JKW, Altstädt V, Schmalz H, Abetz V, and Müller AHE. Polymer 2007;48(9):2700-2719.
22. Kirschnick T, Gottschalk A, Ott H, Abetz V, Puskas J, and Altstädt V. Polymer 2004;45(16):5653-5660.
23. Auschra C and Stadler R. Macromolecules 1993;26(24):6364-6377.
24. Auschra C and Stadler R. Polymer 1993;34(10):2081-2093.
25. Kambour RP, Bendler JT, and Bopp RC. Macromolecules 1983;16(5):753-757.
26. Khatua BB, Lee DJ, Kim HY, and Kim JK. Macromolecules 2004;37(7):2454-2459.
27. Ray SS and Bousmina M. Macromolecular Rapid Communications 2005;26(20):1639-1646.
28. Ray SS, Pouliot S, Bousmina M, and Utracki LA. Polymer 2004;45(25):8403-8413.
29. Chow WS, Mohd-Ishak ZA, Karger-Kocsis J, Apostolov AA, and Ishiaku US. Polymer 2003;44(24):7427-7440.
30. Gültner M, Göldel A, and Pötschke P. Composites Science and Technology 2011;72(1):41-48.
31. Ma PC, Siddiqui NA, Marom G, and Kim JK. Composites Part A: Applied Science and Manufacturing 2010;41(10):1345-1367.
32. Meng L, Fu C, and Lu Q. Progress in Natural Science 2009;19(7):801-810.
33. Albuerne J, Boschetti-de-Fierro A, and Abetz V. Journal of Polymer Science Part B: Polymer Physics 2010;48(10):1035-1046.
34. Suslick KS and Price GJ. Annual Review of Materials Science 1999;29(1):295-326.
35. Zenkel C, Albuerne J, Emmler T, Boschetti-de-Fierro A, Helbig J, and Abetz V. Microchimica Acta 2012;179(1-2):41-48.
36. Wang TL and Tseng CG. Journal of Applied Polymer Science 2007;105(3):1642-1650.
37. Osswald S, Havel M, and Gogotsi Y. Journal of Raman Spectroscopy 2007;38(6):728-736.
38. Wang S, Liang Z, Liu T, Wang B, and Zhang C. Nanotechnology 2006;17(6):1551-1557.
39. Lee YW, Kang SM, Ro YK, Chi YS, Choi I, Hong SP, Yu BC, Paik HJ, and Yun WS. Macromolecular Research 2005;13(4):356-361.
40. Michler GH. Electron Microscopy of Polymers. Berlin Heidelberg: Springer, 2008.
41. Haase A, Hesse P, Brommer L, Jacobs O, Abetz C, Handge UA, Boschetti-de-Fierro A, and Abetz V. Macromolecular Materials and Engineering 2012:n/a-n/a.
42. Wu D, Zhang Y, Zhang M, and Yu W. Biomacromolecules 2009;10(2):417-424.
43. Schmidt LR. Journal of Applied Polymer Science 1979;23(8):2463-2479.
44. Bose S, Bhattacharyya AR, Kodgire PV, Misra A, and Pötschke P. Journal of Applied Polymer Science 2007;106(6):3394-3408.
45. Amr IT, Amer AA, P ST, Harthi MA, Girei SA, Sougrat R, and Atieh MA. Composites Part B: Engineering 2011;42(6):1554-1561.
46. Graebling D, Muller R, and Palierne JF. Macromolecules 1993;26(2):320-329.
47. Bousmina M. Rheologica Acta 1999;38(3):251-254.
48. PrestJr WM and Porter RS. Journal of Polymer Science Part A-2: Polymer Physics 1972;10(9):1639-1655.